Industrial Crops and Products 69 (2015) 80–90

Contents lists available at ScienceDirect

Industrial Crops and Products

journal homepage: www.elsevier.com/locate/indcrop

HPLC-ESI-MS^n characterization of phenolic compounds, terpenoid saponins, and other minor compounds in *Bituminaria bituminosa*

Eulogio J. Llorent-Martínez[a,b,*], Vítor Spínola[a], Sandra Gouveia[c], Paula C. Castilho[a]

[a] Centro de Química da Madeira (CQM), Centro de Ciências Exactas e da Engenharia da Universidade da Madeira, Campus Universitário da Penteada, 9000-390 Funchal, Portugal
[b] Department of Physical and Analytical Chemistry, University of Jaén, Campus Las Lagunillas S/N, E-23071 Jaén, Spain
[c] Department of Chemistry, Umeå University, 901-87 Umeå, Sweden

ARTICLE INFO

Article history:
Received 3 November 2014
Received in revised form 13 January 2015
Accepted 11 February 2015
Available online 18 February 2015

Keywords:
Psoralea bituminosa
Phenolic compounds
HPLC-ESI/MS^n
Tandem mass spectrometry

ABSTRACT

Bituminaria bituminosa is a wild legume that can endure drastic conditions, including contaminated and degraded soils. It has been traditionally used as feeding for livestock, and different uses in folk medicine are known. The chemical composition of leaves and flowers from *B. bituminosa* is presented for the first time. The screening of phytochemical compounds was carried out using high-performance liquid chromatography with electrospray ionization mass spectrometric detection (HPLC-ESI-MS^n). More than 40 compounds were identified or tentatively characterized. A high percentage of the detected compounds corresponded to glycosylated flavonoids, especially from apigenin, although phenolic acids, lignans, and saponins were also identified.

1. Introduction

Bituminaria bituminosa (L.) C.H. Stirton, or *Psoralea bituminosa* L., is a perennial wild legume widely distributed in the Mediterranean basin. Commonly called as "Arabian pea" or "pitch trefoil" it belongs to the Fabaceae family, which comprises a large number of economically important agricultural and food plants, such as soybean, beans, pea, chickpeas, alfalfa, and peanut, among others (Permender et al., 2010).

B. bituminosa is an herbaceous perennial and pubescent plant. Leaves are cauline, pinnately or subdigitately 3-foliolate, linear-lanceolate to broadly-ovate with entire margins. Inflorescence presents several flowers and calyx with long setaceous teeth exceeding the tube (10–15 mm); corolla scarcely exceeding the sharply subulate-tipped calyx-lobes, blue, violet or creamy-white. It blooms between April and August (Press and Short, 2001). When rubbed between the fingers, the foliage emits a characteristic smell of naphta. This strong aroma can be attributed to the combination of phenolics, sulphurated compounds, sesquiterpenes and probably short-chain hydrocarbons (Tava et al., 2007).

One of the main applications of *B. bituminosa* is using it as forage shrub, considering that good forage quality and biomass production have been reported for this species (Pecetti et al., 2007; Ventura et al., 2004). For instance, it is traditionally used for feeding goats in the Canary Islands (Spain) (Sternberg et al., 2006). *B. bituminosa* tolerates drought conditions, and is known for its heavy metal-phytostabilization capacity in contaminated or degraded soils (Martínez-Fernández and Walker, 2012; Martínez-Fernández et al., 2011; Pecetti et al., 2007). Thus, the presence of toxic compounds in this plant can limit its use and has to be taken into account.

In Madeira Island, it is commonly used in folk medicine as a decoction with alcohol and iodine and applied externally for hair restoration. The infusion from fresh leaves is also used for the treatment of fever and urinary infections (Darias et al., 2001; Freitas and Mateus, 2013; Rivera and Obón, 1995).

Previous studies on this species have reported high contents of phytochemicals with pharmaceutical interest, namely furanocoumarins (psoralen and angelicin), pterocarpans (Erybraedin C and bitucarpin A) and flavonoids (daidzin and isoorientin). Good antioxidant and antibacterial activities have also been described for *B. bituminosa* extracts (Azzouzi et al., 2014; Martínez et al., 2010; Maurich et al., 2006; Walker et al., 2012). However, these previous studies were not focused on its phenolic profile.

Phenolic compounds have been used for centuries in different medicinal applications. The antioxidative and pharmacological

* Corresponding author at: University of Jaen, Department of Physical and Analytical Chemistry, Campus Las Lagunillas S/N, E-23071 Jaen, Spain. Tel.: +34 953 211710; fax: +34 953 212940.
E-mail address: ellorent@ujaen.es (E.J. Llorent-Martínez).

http://dx.doi.org/10.1016/j.indcrop.2015.02.014
0926-6690/

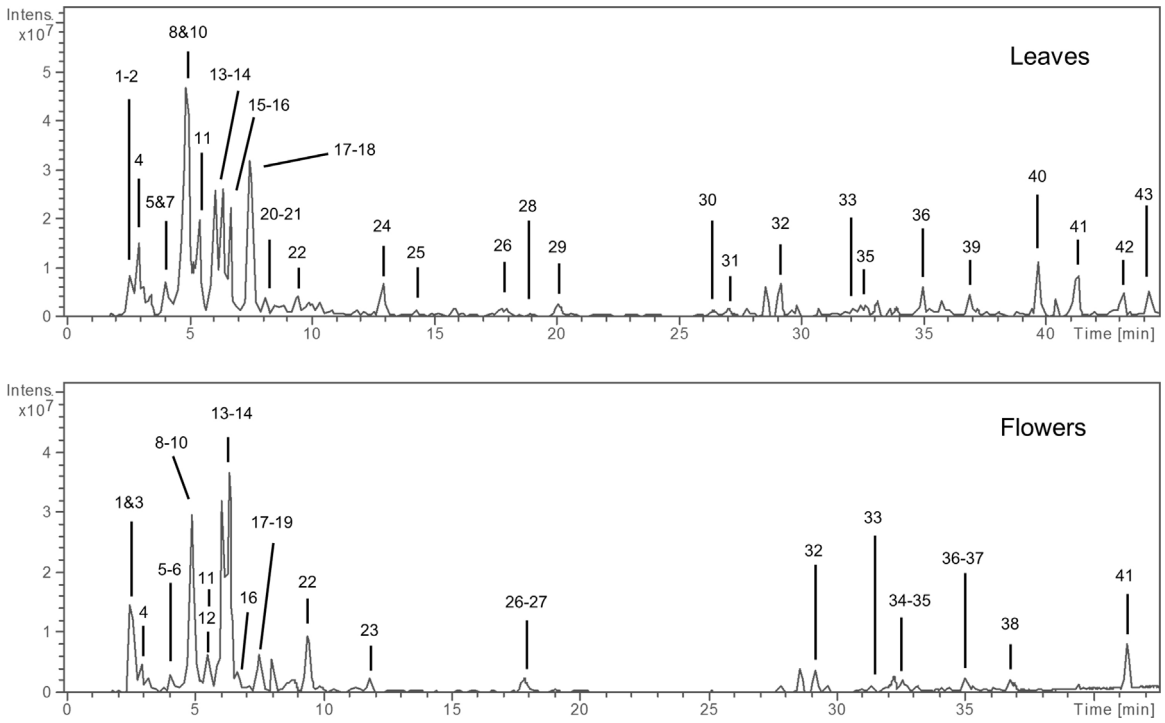

Fig. 1. HPLC-ESI/MS^n base peak chromatograms (BPC) of the methanolic extracts from *B. bituminosa* (leaves and flowers).

properties of medicinal plants are usually related to the presence of phenolic compounds, especially phenolic acids and flavonoids, which are of great interest mainly due to their bioactive functions involved in human health-related issues. Hence, there is a growing interest in substances exhibiting antioxidant properties, which can be used as food or cosmetics components or as specific preventive pharmaceuticals (Gouveia et al., 2013).

In this work, the screening of the chemical composition of leaves and flowers of *B. bituminosa* is presented for the first time, using high-performance liquid chromatography with electrospray ionization mass spectrometric detection (HPLC-ESI-MS^n).

2. Experimental

2.1. Chemicals and reagents

All reagents and standards were of analytical reagent (AR) grade unless stated otherwise. Kaempferol (>99%) was purchased from Acros Organics (Geel, Belgium). Apigenin (≥99%) was obtained from Extrasynthese (Genay, France). Caffeic acid (≥98%) was purchased from Sigma–Aldrich (St. Louis, MO, USA). The methanol (99.9%) used for the extraction of *B. bituminosa* was purchased from Fisher (Lisbon, Portugal). LC–MS grade acetonitrile (CH_3CN) (99%) (LabScan; Dublin, Ireland) and ultrapure water (Milli-Q Waters purification system; Millipore; Milford, MA, USA) were used for HPLC–MS analysis.

2.2. Sample preparation and extraction of phenolic compounds

Samples of *B. bituminosa* were collected in the wild in Madeira Island, in June 2012, with the help of Professor Miguel Menezes de Sequeira from the Biology Department of Madeira University. Vouchers were deposited in the Madeira Botanical Garden Herbarium collection. Specimen collection was performed at full maturity of leaves, in a protected forest area, of restricted human access, and free of contamination from agricultural pesticides or heavy metals from vehicles transit. Leaves and flowers were air-dried separately, ground to powder in a mechanic grinder, and stored at −20 °C until analysis.

The phenolic compounds were extracted by ultrasound-assisted solvent extraction. Briefly, 1 g of dried plant material was extracted with 25 mL of methanol using a sonicator Bandelin Sonorex (Germany) at 35 Hz and 200 W for 60 min (room temperature). Then, chlorophylls were removed by adsorption on activated charcoal and extracts were filtered and concentrated to dryness under reduced pressure in a rotary evaporator (Buchi Rotavapor R-114; USA) at 40 °C. The resulting extracts were stored at −20 °C until further analysis.

2.3. Chromatographic conditions

The HPLC analysis was performed on a Dionex ultimate 3000 series instrument (Thermo Scientific Inc.) coupled to a binary pump, an autosampler and a column compartment (kept at 20 °C). Separation was carried out on a Phenomenex Gemini C_{18} column (5 μm, 250 × 3.0 mm i.d.) using a mobile phase composed by CH_3CN (A) and water/formic acid (0.1%, v/v) at a flow rate of 0.4 mL min^{-1}. The following gradient program was used: 20% A (0 min), 25% A (10 min), 25% A (20 min), 50% A (40 min), 100% A (42–47 min) and 20% A (49–55 min). A solution with concentration (w/v) of 5 mg mL^{-1} was prepared by dissolving the dried extract in the initial HPLC mobile phase. After filtration through 0.45 μm PTFE membrane filters, 10 μL was injected.

For HPLC-ESI-MS^n analysis, a Bruker Esquire model 6000 ion trap mass spectrometer (Bremen, Germany) with an ESI source was used. MS^n analysis was performed in negative and positive mode and scan range was set at m/z 100–1000 with speed of 13,000 Da/s. The conditions of ESI were as follows: drying and nebulizer gas (N_2) flow rate and pressure, 10 mL min^{-1} and 50 psi; capillary temperature, 325 °C; capillary voltage, 4.5 keV; collision gas (He) pressure and energy, 1×10^{-5} mbar and 40 eV. The acquisition of MS^n data was made in auto MS^n mode, with isolation width of 4.0 m/z, and a fragmentation amplitude of 1.0 V (MS^n up to MS^4).

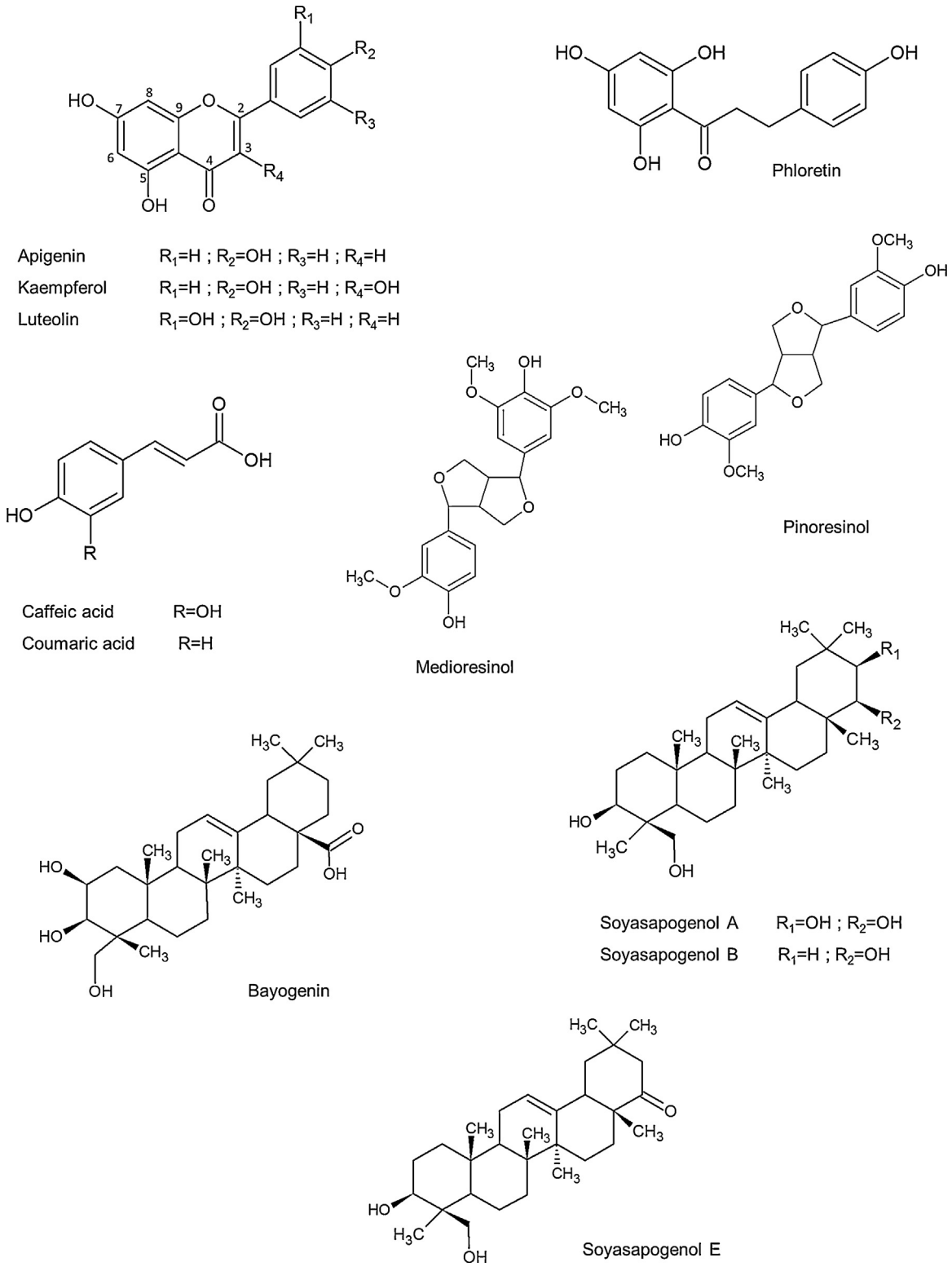

Fig. 2. Chemical structures of the main compounds detected in *B. bituminosa*.

Esquire control software was used for the data acquisition, and Data Analysis software for data processing.

3. Results and discussion

For the analysis of the chemical composition of leaves and flowers by HPLC-ESI-MS^n, both the positive and negative ionization modes were used. Two independent assays were performed for each sample, and no relevant variations were observed regarding the nature of the detected fragments and their relative intensities. The base peak chromatograms of the methanolic extracts are shown in Fig. 1.

An essential step in these analyses was to determine the molecular weight of each compound. In general, in the negative ionization mode (ESI^-) MS^1 spectrum, the most intense peak corresponded

to the deprotonated molecular ion $[M–H]^-$; this permitted to perform MS^n analysis. The mass spectra of the conjugated phenolic compounds showed the aglycone ion as a result of the loss of sugar moieties like hexosyl, deoxyhexosyl, pentosyl, rutinosyl, and glucuronyl (−162, −146, −132, −308, and −176 Da, respectively). Mass spectra data from the positive ionization (ESI^+) mode was used for confirmation purposes. Compounds were numbered by their order of elution and this numeration was kept identical for leaves and flowers. The structures of the most relevant compounds are shown in Fig. 2.

3.1. Phenolic acids

Compound 14, with an $[M–H]^-$ ion at m/z 731, suffered a neutral loss of 366 Da in MS^2, yielding a fragment ion at m/z 365, so it was identified as a dimer. It was characterized as a caffeoyl derivative due to the loss of 162 Da, and a signal of low abundance at m/z 179 in MS^3 experiments (Kammerer et al., 2004). The MS^3 fragment ion at m/z 203 was identified as tryptophan, taking into account the $MS^4[731 \rightarrow 365 \rightarrow 203]$ fragment ion at m/z 159, characteristic of tryptophan (Kramer et al., 2013). Hence, compound 14 was characterized as caffeoyl-*N*-tryptophan, a substance previously found in green coffee and coriander (Barros et al., 2012). This compound was observed in both leaves and flowers.

Compound 26 exhibited an $[M–H]^-$ ion at m/z 561, and presented the $MS^3[561–439]$ base peak at m/z 163, which exhibited a fragment ion at m/z 119 after further fragmentation. This $163 \rightarrow 119$ fragmentation is typical from coumaric acid (Gruz et al., 2008). Without further information this compound, detected in leaves and flowers, was just characterized as a derivative.

Compound 28 was identified as hydroxybenzoic acid based on its deprotonated molecular ion at m/z 137, and characteristic fragment ion at m/z 93.

Compound 30, with an $[M–H]^-$ ion at m/z 511, suffered the neutral loss of 146 Da (rhamnoside) to yield a fragment ion at m/z 365, which showed a fragmentation pattern similar to compound 14. This compound was characterized as caffeoyl-*N*-tryptophan-rhamnoside and, to our knowledge, is here reported for the first time. It was detected in leaves, but not in flowers Tables 1 and 2.

3.2. Flavonoids

Several derivatives of apigenin were detected in the methanolic extracts of leaves and flowers. All these flavonoids were identified as glycosides containing one or more sugar moieties. Both *C*-glycosylated flavonoids and *O*-glycosylated flavonoids were detected. These two groups of flavonoids are easily distinguished based on the MS^n fragmentation pattern. The carbon–carbon bond of *C*-glycosylated flavonoids is resistant to rupture, so the main cleavages are at the bonds of the sugar. However, the sugar moieties are easily lost by neutral losses in *O*-glycosylated flavonoids (Jin et al., 2008).

The *O*-glycosylated derivative of apigenin was compound 23, detected only in flowers. This compound displayed an $[M–H]^-$ ion at m/z 431, and its MS^2 spectrum exhibited a fragment ion at m/z 269, indicating the neutral loss of 162 Da (hexoside). Further fragmentation of the ion at m/z 269 showed characteristic fragments of apigenin at m/z 225 and 151. Therefore compound 23 was characterized as apigenin-7-*O*-hexoside (Gouveia and Castilho, 2012; Qiao et al., 2011).

All the *C*-glycosylated derivatives of apigenin were detected in leaves and flowers. Compounds 4 and 10 showed $[M–H]^-$ ions at m/z 563. Both compounds have been previously described by our group (Gouveia and Castilho, 2013). Their MS^2 fragmentation revealed a behavior typical of the asymmetrical di-*C*-glycosides, with fragment ions at $[M–H–210]^-$, $[M–H–90]^-$, and $[M–H–60]^-$ at m/z 353, 473, and 503, respectively. The neutral loss of 60 Da indicated the presence of a pentose moiety. Considering that 6-*C*-pentoside-8-*C*-hexoside elutes before the isomer 6-*C*-hexoside-8-*C*-pentoside, compounds 4 and 10 were characterized as apigenin 6-*C*-pentoside-8-*C*-hexoside and apigenin-6-*C*-hexoside-8-*C*-pentoside, respectively.

Compound 5 was characterized as vicenin-2 (apigenin 6,8-di-*C*-hexoside) based on bibliographic information (Ferreres et al., 2003; Zhang et al., 2011). It showed an $[M–H]^-$ ion at m/z 593, and presented the typical di-*C*-glycosyl flavone MS^2 fragmentation pattern of $[M–H–18]^-$, $[M–H–90]^-$, $[M–H–120]^-$, $[aglycone+113]^-$, and $[aglycone+83]^-$ at m/z 575, 503, 473, 383, and 353, respectively.

Compound 13, with an $[M–H]^-$ ion at m/z 593, displayed MS^2 base peak at m/z 413 and $MS^3[593 \rightarrow 413]$ base peak at m/z 293. This fragmentation pattern has been previously described for other apigenin derivative, isovitexin-2″-*O*-glucoside (Jung et al., 2013). These authors also described the fragmentation observed using the positive ionization mode, which showed an $[M+H]^+$ ion at m/z 595, with main MS^n fragment ions at m/z 433 and 367. This pattern was also observed for compound 13, so confirming the identification. It was detected in leaves and flowers.

Compound 15, only detected in leaves, was tentatively characterized as apigenin-*C*-hexoside-*O*-pentoside according to bibliographic data (Hauck et al., 2014; Santos et al., 2014). Compound 16, with an $[M–H]^-$ ion at m/z 577 and main MS^n fragment ions at m/z 413 and 293, was characterized as vitexin rhamnoside (Slimestad, 2003); it was detected in leaves and flowers.

Compound 18 exhibited an $[M–H]^-$ ion at m/z 431, and its MS^2 spectrum showed typical fragment ions of *C*-glycosides at m/z 311 and 341, corresponding to $[M–H–120]^-$ and $[M–H–90]^-$, respectively. Considering the guidelines for the identification of isomeric mono-*C*-glycosides flavonoids (Waridel et al., 2001), the compound was identified as a *C*-8 flavonoid, since the MS^2 spectrum did not show the loss of water molecules, which is representative of *C*-6 isomers. Considering bibliographic data, compound 18 was identified as apigenin-8-*C*-hexoside (Gouveia and Castilho, 2011).

Compound 7, with $[M–H]^-$ ion at m/z 579, presented the typical fragmentation pattern of di-*C*-asymmetric glycosyl flavones (Ferreres et al., 2003), with fragments at m/z 561 $[M–H–18]^-$, 519 $[M–H–60]^-$, 489$[M–H–90]^-$, 459 $[M–H–120]^-$, and 429 $[M–H–150]^-$. For the identification of the aglycone (A), the fragments at m/z 399 [A+113] and 369 [A+83] were considered, yielding a molecular weight of 286 Da for the aglycone, which could correspond to kaempferol or luteolin. Considering scientific bibliography (Hauck et al., 2014; Simirgiotis et al., 2013), this compound was identified as luteolin-*C*-hexoside-*C*-pentoside

Compound 8, with an $[M–H]^-$ ion at m/z 435, exhibited MS^2 fragment ions at m/z 345 $[M–H–90]^-$, and 315 $[M–H–120]^-$. This fragmentation pattern is consistent with *C*-glycosidic flavonoids (Waridel et al., 2001). Although the aglycone is not usually identified in *C*-glycosylated flavonoids, its molecular weight may be 274 Da (M-162 Da (hexoside)), which would correspond to the presence of the dihydrochalcone phloretin. In this case, the positive ionization mode of compound 8 exhibited an $[M+H]^+$ ion at m/z 437, with MS^2 base peak at m/z 317. This fragmentation pattern has been previously described for nothofagin (phloretin 3′-*C*-glycoside) (Kazuno et al., 2005).

Compound 11 was characterized as isoorientin (luteolin 6-*C*-glucoside) considering bibliographic data (Waridel et al., 2001). This compound exhibited an $[M–H]^-$ ion at m/z 447, with MS^2 fragment ions at m/z 357 and 327, and $MS^3[447 \rightarrow 327]$ base peak at m/z 299. This fragmentation pattern was consistent with luteolin-*C*-hexoside. The differentiation between 6-*C* and 8-*C*-glycosidic flavonoids was made considering the MS^2 fragment ions at m/z 429 ($[M–H–18]^-$) and 411 ($[M–H–36]^-$), and MS^3 fragment ion at m/z 309, which are characteristic of isoorientin and are absent

Table 1
Characterization of the methanolic extracts of leaves from *B. bituminosa*.

No.	t_R (min)	$[M–H]^-$ (m/z)	m/z (% Base peak)	Assigned identification	Ref.
1	2.6	683	MS^2 [683]: 503 (1.5), 342 (12.1), 341 (100) MS^3 [683 → 341]: 179 (100), 161 (22.7), 143 (14.4), 131 (11.5), 119 (29.0), 101 (15.1) MS^4 [683 → 341 → 179]: 149 (100), 131 (73.1), 125 (30.9), 119 (72.1), 89 (38.5), 71 (44.5)	Hexose polymer	(Brudzynski and Miotto, 2011)
2	2.6	457	MS^2 [457]: 342 (10.1), 341 (100) MS^3 [457 → 341]: 179 (100), 161 (62.7), 143 (68.2), 131 (14.3), 113 (36.9), 101 (40.2) MS^4 [457 → 341 → 179]: 143 (100), 89 (33.0), 71 (35.1)	Malic acid dihexoside	–
4	3.0	563	MS^2 [563]: 545 (18.1), 503 (18.5), 473 (78.7), 443 (100), 383 (73.8), 353 (96.7) MS^3 [563 → 353]: 326 (26.3), 325 (100), 298 (18.6), 297 (62.5) MS^4 [563 → 353 → 325]: 298 (23.3), 297 (100)	Apigenin-6-*C*-pentoside-8-*C*-hexoside	(Gouveia and Castilho, 2013)
5	4.1	593	MS^2 [593]: 575 (4.8), 503 (39.4), 474 (21.7), 473 (100), 383 (39.7), 353 (60.7) MS^3 [593 → 473]: 383 (24.4), 354 (17.8), 353 (100) MS^4 [593 → 473 → 353]: 325 (100), 298 (18.2), 297 (61.8)	Apigenin-6,8-di-*C*-glucoside (Vicenin-2)	(Zhang et al., 2011)
7	4.4	579	MS^2 [579]: 561 (13.2), 519 (6.4), 489 (100), 459 (91.9), 429 (29.1), 399 (46.2), 369 (28.4) MS^3 [579 → 489]: 429 (10.8), 411 (17.7), 399 (92.7), 369 (100)	Luteolin-*C*-hexoside-*C*-pentoside	–
8	4.7	435	MS^2 [435]: 345 (34.2), 316 (15.0), 315 (100) MS^3 [435 → 315]: 298 (11.4), 297 (66.0), 243 (19.1), 109 (50.7), 191 (100), 190 (27.2), 162 (11.8), 151 (28.1) MS^4 [435 → 315 → 191]: 163 (100), 162 (80.8), 148 (13.9), 137 (16.1), 135 (12.2)	Phloretin-*C*-hexoside (Nothofagin)	(Kazuno et al., 2005)
10	4.9	563	MS^2 [563]: 503 (20.0), 473 (70.6), 443 (100), 383 (58.8), 353 (81.2) MS^3 [563 → 443]: 383 (27.7), 354 (13.7), 353 (100) MS^4 [563 → 443 → 353]: 326 (22.4), 325 (100), 298 (13.6), 297 (63.4)	Apigenin-6-*C*-hexoside-8-*C*-pentoside	(Gouveia and Castilho, 2013)
11	5.5	447	MS^2 [447]: 429 (25.2), 411 (2.3), 358 (17.1), 357 (100), 328 (18.1), 327 (95.3) MS^3 [447 → 357]: 340 (22.4), 339 (100), 311 (19.2), 297 (76.2), 285 (61.8) MS^3 [447 → 327]: 309 (8.5), 301 (13.0), 299 (100), 298 (14.3), 284 (17.3) MS^4 [447 → 357 → 285]: 243 (66.5), 241 (100), 211 (68.2), 199 (76.7), 175 (33.5), 151 (10.8), 107 (52.6) MS^4 [447 → 357 → 339]: 312 (31.1), 311 (100) MS^4 [447 → 327 → 299]: 255 (100), 242 (85.4), 240 (14.0), 209 (54.7), 135 (55.7)	Luteolin 6-*C*-hexoside (isoorientin)	(Waridel et al., 2001)
13	6.0	593	MS^2 [593]: 575 (10.6), 504 (10.9), 503 (54.3), 474 (14.8), 473 (63.3), 414 (17.9), 413 (100), 383 (54.3), 293 (29.3) MS^3 [593 → 413]: 294 (17.6), 293 (100) MS^3 [593 → 473]: 413 (15.4), 384 (13.5), 383 (100) MS^4 [593 → 413 → 293]: 173 (100) MS^4 [593 → 473 → 383]: 368 (26.3), 355 (61.0), 340 (22.3), 313 (18.7), 311 (100)	Isovitexin-2″-*O*-glucoside	(Jung et al., 2013)
14	6.2	731	MS^2 [731]: 366 (12.4), 365 (100) MS^3 [731 → 365]: 203 (100), 179 (1.7), 159 (56.3) MS^4 [731 → 365 → 203]: 159 (100)	Caffeoyl-*N*-tryptophan dimer	(Barros et al., 2012)
15	6.5	563	MS^2 [563]: 443 (9.8), 414 (25.6), 413 (100), 341 (11.2), 294 (16.4), 293 (73.9) MS^3 [563 → 413]: 294 (20.6), 293 (100) MS^4 [563 → 413 → 293]: 293 (74.8), 247 (15.2), 175 (100), 173 (17.0)	Apigenin-*C*-hexoside-*O*-pentoside	(Hauck et al., 2014; Santos et al., 2014)
16	6.7	577	MS^2 [577]: 457 (15.4), 414 (17.7), 413 (100), 294 (10.1), 293 (60.1) MS^3 [577 → 413]: 294 (15.8), 293 (100) MS^4 [577 → 413 → 293]: 293 (100), 278 (13.3), 276 (11.6), 275 (11.3), 251 (13.9), 149 (21.0), 221 (12.3), 175 (46.2), 173 (35.0), 163 (17.5)	Apigenin 8-*C*-glucoside rhamnoside (vitexin rhamnoside)	(Slimestad, 2003)
17	7.5	425	MS^2 [425]: 277 (12.3), 263 (73.9), 245 (100), 183 (14.4), 173 (13.4) MS^3 [425 → 245]: 201 (41.3), 183 (94.9), 173 (100), 171 (11.7), 147 (18.4), 131 (50.1) MS^4 [425 → 245 → 183]: 143 (100)	Unknown	–
18	7.6	431	MS^2 [431]: 341 (33.6), 312 (22.1), 311 (100) MS^3 [431 → 311]: 284 (28.3), 283 (100) MS^4 [431 → 311 → 283]: 283 (83.6), 212 (100), 197 (78.6), 183 (71.0), 165 (53.8), 163 (48.6), 119 (94.9)	Apigenin-8-*C*-hexoside	(Gouveia and Castilho, 2011)
20	8.2	461	MS^2 [461]: 443 (2.4), 371 (25.0), 342 (20.4), 341 (100) MS^3 [461 → 341]: 313 (20.1), 299 (22.0), 298 (100) MS^4 [461 → 341 → 298]: 298 (100), 269 (34.1)	6-*C*-glycosylated flavonoid	–
21	8.4	447	MS^2 [447]: 286 (11.5), 285 (100) MS^3 [447 → 285]: 243 (38.2), 241 (85.1), 217 (66.5), 175 (100), 151 (20.7)	Luteolin-*O*-hexoside	–

22	9.5	593	MS^2 [593]: 286 (16.2), 285 (100) MS^3 [593 → 285]: 267 (30.3), 257 (100), 255 (23.3), 241 (57.5), 229 (47.3), 213 (41), 151 (23.9) MS^4 [593 → 285 → 257]: 255 (69.0), 229 (100), 213 (43.2), 169 (12.7)	Kaempferol-*O*-rutinoside	(Ye et al., 2005)
24	13.0	663	MS^2 [663]: 632 (29.0), 631 (88.3), 588 (36.4), 587 (100), 569 (19.7) MS^3 [663 → 587]: 570 (28.2), 569 (100), 557 (13.2), 327 (15.8) MS^4 [663 → 587 → 569]: 551 (57.9), 509 (43.0), 446 (39.2), 327 (100), 309 (32.2)	Unknown	–
25	14.4	561	MS^2 [561]: 544 (10.2), 543 (38.3), 523 (17.5), 358 (19.8), 357 (100) MS^3 [561 → 357]: 342 (20.9), 327 (22.4), 151 (100), 136 (36) MS^4 [561 → 357 → 151]: 136 (100)	Pinoresinol-*O*-acetylhexoside	–
26	17.8	561	MS^2 [561]: 440 (20.9), 439 (100), 163 (18.6) MS^3 [561 → 439]: 277 (17.4), 236 (28.3), 165 (11.7), 164 (50.3), 163 (100) MS^4 [561 → 439 → 163]: 119 (100)	Coumaric acid derivative	–
28	19.0	137	MS^2 [137]: 93 (100)	Hydroxybenzoic acid	*(Gruz et al., 2008)*
29	20.0	393	MS^2 [393]: 231 (100) MS^3 [393 → 231]: 187 (100), 132 (2.9) MS^4 [393 → 231 → 187]: 132 (100)	Unknown	–
30	26.1	511	MS^2 [511]: 365 (15.2), 265 (11.7), 203 (100), 163 (28.5) MS^3 [511 → 203]: 161 (25.1), 159 (100)	Caffeoyl-*N*-tryptophan-rhamnoside	–
31	26.8	647	MS^2 [647]: 615 (49.8), 572 (36), 571 (100), 399 (22.8) MS^3 [647 → 571]: 512 (29), 447 (28), 446 (49.9), 327 (100), 309 (31.9) MS^4 [647 → 571 → 327]: 309 (100), 297 (51.6), 291 (21), 281 (77), 280 (32.7)	Unknown	–
32	29.1	973	MS^2 [973]: 955 (100), 929 (1.4), 911 (66.3), 827 (10.7), 809 (2.7), 783 (3.2), 765 (51.7), 665 (1.6), 647 (57.7), 629 (19), 603 (13.4), 557 (61.5), 489 (26.4) MS^3 [973 → 955]: 911 (36.4), 765 (48.0), 557 (100), 489 (12.1)	6-deoxyhexose-hexoside-uronic acid-aglycone D	(Pollier et al., 2011)
33	31.7	327	MS^2 [327]: 291 (56.0), 229 (100), 211 (51.9), 209 (10.8), 171 (62.1), 165 (15.2) MS^3 [327 → 229]: 211 (100), 209 (64.4), 193 (23.5), 165 (18.0), 155 (22.1), 125 (9.6)	Oxo-dihydroxy-octadecenoic acid	(Spínola et al., 2014; Van Hoyweghen et al., 2014)
35	32.7	971	MS^2 [971]: 953 (30.5), 927 (9.6), 909 (100), 825 (2.7), 763 (31.1), 645 (88.9), 627 (4.7), 601 (16.5), 555 (18.1), 487 (11.8), 469 (28.9) MS^3 [971 → 909]: 763 (100), 745 (9.3), 601 (49.5), 487 (14.8), 439 (3.8)	6-deoxyhexose-hexose-uronic acid-bayogenin	(Pollier et al., 2011)
36	34.9	957	MS^2 [957]: 939 (100), 895 (38.4), 811 (14.1), 767 (9.9), 749 (58.2), 631 (43.2), 613 (15.5), 541 (63.3), 473 (13.8) MS^3 [957 → 939]: 895 (45.9), 749 (64.4), 613 (24.2), 541 (100), 473 (17.3)	6-deoxyhexose-hexose-uronic acid-soyasapogenol A	(Pollier et al., 2011)
39	36.9	327	MS^2 [327]: 309 (100), 291 (30.5), 251 (31.8), 209 (24.2) MS^3 [327 → 309]: 291 (100), 235 (10.6) MS^4 [327 → 309 → 291]: 273 (90.2), 247 (100), 235 (68.3), 219 (48.6), 123 (61.2)	Trihydroxy-octadienoic acid	(Mohn et al., 2009)
40	39.6	231	MS^2 [231]: 188 (12.8), 187 (100) MS^3 [231 → 187]: 132 (100)	Unknown	
41	41.1	941	MS^2 [941]: 923(100), 879 (51.9), 795 (11.3), 751 (9.7), 733 (68.8), 633 (3.6), 615 (58.2), 597 (25.4), 525 (69.8), 457 (15.6) MS^3 [941 → 923]: 879 (42.5), 733 (69), 597 (20.5), 525 (100), 457 (11.7)	3-rhamnose-galactose-glucuronic acid-soyasapogenol B	(Pollier et al., 2011)
42	43	337	MS^2 [337]: 319 (33.7), 161 (17.5), 149 (100) MS^3 [337 → 149]: 123 (100), 121 (5.0), 119 (41.5)	Unknown	
43	44	939	MS^2 [939]: 921 (100), 877 (59.2), 793 (14.5), 749 (10.7), 731 (65.2), 613 (52.3), 595 (26.4), 523 (69.6), 455 (28.3) MS^3 [939 → 921]: 877 (55.6), 731 (96.8), 595 (38.1), 523 (100), 455 (18.5)	6-deoxyhexose-hexose-uronic acid-soyasapogenol E	(Pollier et al., 2011)

Table 2
Characterization of the methanolic extracts of flowers from *B. bituminosa*.

No.	t_R(min)	[M–H]$^-$(m/z)	m/z (% Base peak)	Assigned identification	Ref.
1	2.6	683	MS^2 [683]: 503 (1.3), 342 (14.4), 341 (100) MS^3 [683 → 341]: 179 (100), 161 (20.1), 143 (21.4), 119 (26.2), 113 (49.8) MS^4 [683 → 341 → 179]: 143 (100), 131 (73.6), 119 (48.1), 113 (27.7), 89 (38.5)	Hexose polymer	(Brudzynski and Miotto, 2011)
3	2.6	473	MS^2 [473]: 342 (9.3), 341 (100) MS^3 [473 → 341]: 179 (100), 161 (12.5), 143 (24.2), 119 (20.7), 113 (14.7) MS^4 [473 → 341 → 179]: 161 (89.4), 143 (100), 131 (36.2), 119 (85.8), 113 (86.8), 101 (65.9)	Trisaccharide (pentose + 2 hexoses)	–
4	3.0	563	MS^2 [563]: 503 (18.2), 473 (66.7), 443 (100), 383 (63.4), 353 (89.8) MS^3 [563 → 443]: 383 (31.1), 354 (18.5), 353 (100) MS^4 [563 → 443 → 353]: 326 (64.7), 325 (100), 297 (25.2), 265 (50.2)	Apigenin-6-*C*-pentoside-8-*C*-hexoside	(Gouveia and Castilho, 2013)
5	4.1	593	MS^2 [593]: 575 (13.3), 503 (30.7), 474 (24.4), 473 (100), 383 (27.7), 353 (58.3) MS^3 [593 → 473]: 383 (18.4), 354 (21.3), 353 (100) MS^4 [593 → 473 → 353]: 326 (26.7), 325 (100), 307 (35.6), 298 (47.7), 297 (95.2), 283 (23.8), 282 (11.8), 197 (15.3), 189 (12.4), 117 (24.6)	Apigenin-6,8-di-*C*-hexoside (Vicenin-2)	(Zhang et al., 2011)
6	4.1	431	MS^2 [431]: 369 (45.7), 329 (100), 271 (45.6), 203 (47.2), 125 (73.9) MS^3 [431 → 271]: 256 (18.7), 243 (30.2), 227 (45.2), 203 (25.4), 161 (100) MS^3 [431 → 329]: 233 (17.0), 221 (24.7), 203 (29.3), 179 (22.4), 125 (100) MS^4 [431 → 329 → 125]: 97 (100)	Unknown	–
8	4.7	435	MS^2 [435]: 345 (34.2), 316 (15.0), 315 (100) MS^3 [435 → 315]: 298 (15.1), 297 (41.2), 271 (10.4), 243 (18.4), 209 (100), 191 (22.1), 191 (73.4), 190 (41.3), 163 (25.9), 151 (10.1) MS^4 [435 → 315 → 209]: 191 (100), 163 (47.8)	Phloretin-*C*-hexoside (nothofagin)	*(Kazuno et al., 2005)*
9	4.7	387	MS^2 [387]: 369 (11.1), 208 (10.5), 207 (100), 164 (11.2), 163 (72.0) MS^3 [387 → 207]: 163 (100)	Medioresinol	(Ozarowski et al., 2013)
10	4.9	563	MS^2 [563]: 503 (28.5), 473 (76.0), 443 (98.5), 383 (56.8), 353 (100) MS^3 [563 → 353]: 326 (19.1), 325 (100), 297 (39.3) MS^3 [563 → 443]: 383 (29.5), 354 (30.8), 353 (100) MS^4 [563 → 353 → 325]: 298 (41.3), 297 (100) MS^4 [563 → 443 → 353]: 326 (31.5), 325 (100), 297 (59.6)	Apigenin-6-*C*-hexoside-8-*C*-pentoside	(Gouveia and Castilho, 2013)
11	5.5	447	MS^2 [447]: 429 (25.6), 411 (4.1), 358 (11.1), 357 (100), 328 (11.6), 327 (89.8) MS^3 [447 → 327]: 327 (21.4), 309 (2.2), 300 (24.7), 299 (100), 284 (15) MS^4 [447 → 327 → 299]: 256 (76.7), 243 (90.3), 229 (78.3), 212 (100)	Luteolin 6-*C*-hexoside (isoorientin)	(Waridel et al., 2001)
12	5.6	449	MS^2 [449]: 288 (12.8), 287 (100), 269 (35.7), 259 (56.4) MS^3 [449 → 287]: 260 (12.0), 259 (100), 243 (17.3), 201 (8.0), 125 (4.0) MS^4 [449 → 287 → 259]: 215 (100), 173 (35.8), 165 (33.2), 151 (32.2), 125 (88.2)	Dihydrokaempferol-*O*-hexoside	(Fischer et al., 2011)
13	6.0	593	MS^2 [593]: 575 (2.4), 503 (54.3), 473 (63.3), 414 (17.9), 413 (100), 383 (12.3), 293 (43.1) MS^3 [593 → 413]: 294 (25.3), 293 (100) MS^4 [593 → 413 → 293]: 293 (100), 173 (11.9)	Isovitexin-2″-*O*-glucoside	(Jung et al., 2013)
14	6.2	731	MS^2 [731]: 366 (12.4), 365 (100) MS^3 [731 → 365]: 203 (100), 179(2.2), 159 (56.3) MS^4 [731 → 365 → 203]: 159 (100)	Caffeoyl-*N*-tryptophan	(Barros et al., 2012)
16	6.7	577	MS^2 [577]: 457 (18.4), 414 (23.7), 413 (100), 367 (25.1), 293 (64.6) MS^3 [577 → 413]: 294 (13.9), 293 (100) MS^4 [577 → 413 → 293]: 293 (35.7), 249 (100), 175 (24.1)	Vitexin rhamnoside	(Slimestad, 2003)

17	7.5	425	MS^2 [425]: 263 (61.7), 245 (100), 191 (15.4), 173 (20.4) MS^3 [425 → 245]: 201 (64.1), 183 (79.3), 173 (100), 171 (47.9), 131 (35.9)	Unknown	–
18	7.6	431	MS^2 [431]: 341 (32.2), 312 (20.0), 311 (100) MS^3 [431 → 311]: 284 (19.9), 283 (100) MS^4 [431 → 311→283]: 239 (96.1), 209 (100), 183 (60.7), 165 (90.8), 163 (49.7)	Apigenin-8-*C*-hexoside	(Gouveia and Castilho, 2011)
19	7.7	371	MS^2 [371]: 249 (100) MS^3 [371 → 249]: 231 (23.1), 175 (5.4), 113 (100), 111 (8.3)	Unknown	
22	9.5	593	MS^2 [593]: 286 (16.2), 285 (100) MS^3 [593 → 285]: 267 (30.3), 257 (100), 241 (57.5), 229 (41.8), 213 (35.3) MS^4 [593 → 285 → 257]: 255 (69.0), 239 (49.5), 229 (100), 213 (43.2), 163 (45.6)	Kaempferol-*O*-rutinoside	(Ye et al., 2005)
23	11.8	431	MS^2 [431]: 270 (16.6), 269 (100) MS^3 [431 → 269]: 269 (63.9), 268 (82.5), 227 (41.6), 225 (49.0) 151 (100) MS^4 [431 → 269 → 225]: 197 (100)	Apigenin-7-*O*-hexoside	(Gouveia and Castilho, 2012)
26	17.8	561	MS^2 [561]: 440 (20.9), 439 (100), 163 (18.6) MS^3 [561 → 439]: 277 (17.4), 236 (28.3), 165 (11.7), 164 (50.3), 163 (100) MS^4 [561 → 439 → 163]: 119 (100)	Coumaric acid derivative	–
27	17.8	521	MS^2 [521]: 400 (15.7), 399 (100) MS^3 [521 → 399]: 179 (14.6), 177 (27.0), 163 (10.5), 153 (23.3), 152 (100), 147 (12.9) MS^4 [521 → 399 → 152]: 125 (36.4), 108 (100)	Unknown	–
32	29.1	973	MS^2 [973]: 955 (100), 911 (66.3), 827 (14.1), 809 (2.0), 783 (6.0), 765 (51.7), 665 (1.7), 647 (57.7), 629 (24.8), 603 (9.6), 557 (61.5), 489 (18.8) MS^3 [973 → 955]: 911 (36.4), 765 (48.0), 629 (73.5), 557 (100), 489 (12.6)	6-Deoxyhexose-hexoside-uronic acid-aglycone D	(Pollier et al., 2011)
33	31.7	327	MS^2 [327]: 291 (34.1), 229 (74.1), 211 (47.2), 209 (28.9), 171 (100) MS^3 [327 → 171]: 153 (100)	Oxo-dihydroxy-octadecenoic acid	(Spínola et al., 2014; Van Hoyweghen et al., 2014)
34	32.3	673	MS^2 [673]: 551 (100), 475 (54.3), 265 (28.9), 197 (35.2) 189 (10.3) MS^3 [673 → 551]: 353 (12.4), 265 (100), 251 (34.7), 237 (90.9), 222 (23.7) MS^4 [673 → 551 → 265]: 222 (61.8), 196 (94.1), 153 (100)	Unknown	–
35	32.7	971	MS^2 [971]: 953 (24.9), 927 (5.5), 909 (100), 825 (3.3), 763 (36.6), 645 (87.7), 627 (5.6), 601 (24.8), 555 (12), 487 (10.7) MS^3 [971 → 909]: 763 (100), 745 (5.7), 601 (40.1), 583 (6.9), 487 (15.2)	6-Deoxyhexose-hexose-uronic acid-bayogenin	(Pollier et al., 2011)
36	34.9	957	MS^2 [957]: 939 (100), 895 (36.7), 811 (11.2), 767 (5.2), 749 (35.4), 631 (35.9), 613 (12.7), 541 (38.5), 473 (12.2) MS^3 [957 → 939]: 895 (45.9), 749 (100), 613 (29.1), 541 (57.4), 473 (11.2)	6-Deoxyhexose-hexose-uronic acid-soyasapogenol A	(Pollier et al., 2011)
37	34.9	329	MS^2[329]: 311 (25.7), 293 (21), 229 (100), 211 (81.4), 171 (40) MS^3[329 → 229]: 211 (100), 209 (67.1), 155 (47.2), 125 (39.6) MS^4 [329 → 229 → 211]: 193 (100)	Trihydroxy-octadecenoic acid	(Van Hoyweghen et al., 2014)
38	36.6	287	MS^2 [287]: 285 (34.9), 270 (25.5), 269 (100), 241 (30.0), 141 (12.1) MS^3 [287 → 269]: 267 (48.9), 251 (100), 235 (31.2), 185 (43.3), 155 (30.5)	Unknown	–
41	41.2	941	MS^2 [941]: 923(100), 879 (39.1), 795 (18.7), 751 (2.8), 733 (57.7), 633 (2.7), 615 (39.6), 597 (14.9), 525 (78.3), 457 (15.0) MS^3 [941 → 923]: 879 (50.5), 733 (41.5), 597 (43.9), 525 (100), 457 (10.6)	3-Rhamnose-galactose-glucuronic acid-soyasapogenol B	(Pollier et al., 2011)

in orientin (luteolin 8-*C*-glucoside). In addition, the 6-*C*-glucoside shows base peak at m/z 357, whereas the 8-*C*-glucoside presents base peak at m/z 327. This compound had been previously reported in *B. bituminosa* aerial parts (Azzouzi et al., 2014).

Compound 12, only detected in flowers, exhibited an $[M–H]^-$ ion at m/z 449. It suffered the neutral loss of 162 Da (hexoside) in MS^2, yielding the aglycone at m/z 287. The aglycone was characterized as dihydrokaempferol, due to the $MS^3[449 \rightarrow 287]$ base peak at m/z 259 (Fischer et al., 2011). Hence, this compound was identified as dihydrokaempferol-*O*-hexoside.

Compound 20 displayed the deprotonated molecular ion at m/z 461, and exhibited MS^2 fragment ions at m/z 443, 371, and 341, corresponding to $[M–H–18]^-$, $[M–H–90]^-$, and $[M–H–120]^-$, respectively. This fragmentation pattern is consistent with 6-*C* glycosylated flavonoids (Waridel et al., 2001), due to the $[M–H–18]^-$ ion, which is absent in 8-*C* glycosylated flavonoids. Taking into account bibliographic data, this compound could be diosmetin-6-*C*-hexoside (Zhang et al., 2011) or isoscoparin (chrysoeriol-6-*C*-hexoside) (Mohn et al., 2009). Without any further information, compound 20 was tentatively characterized as a 6-*C*-glycosylated flavonoid. This flavonoid was only observed in extracts from leaves.

Compound 21 was identified as a luteolin-*O*-hexoside. It displayed $[M–H]^-$ ion at m/z 447, and suffered the neutral loss of 162 Da (hexoside) to yield a fragment ion at m/z 285, which exhibited a fragmentation pattern similar to luteolin (m/z 243, 241, and 151).

Compound 22 displayed the deprotonated molecular ion at m/z 593, and suffered the neutral loss of 308 Da (rutinoside) in MS^2, yielding the aglycone at m/z 285. The aglycone was identified as kaempferol (March and Miao, 2004; March and Miao, 2004). Therefore this compound, detected in extracts from leaves and flowers, was identified as kaempferol rutinoside.

Compound 29 displayed an $[M–H]^-$ at m/z 393, and suffered the neutral loss of 162 Da (hexoside), yielding the aglycone at m/z 231. This aglycone was later detected as compound 40. However, the aglycone could not be identified due to the lack of bibliographic data.

3.3. Lignans

Compound 9, with an $[M–H]^-$ ion at m/z 387 and main MS^2 fragment ions at m/z 207 and 163, was tentatively characterized as the phenolic lignan medioresinol (Ozarowski et al., 2013). This lignan was found only in the methanolic extracts from flowers.

Compound 25 displayed the deprotonated molecular ion at m/z 561, and showed a neutral loss of 204 Da to yield the product ion at m/z 357; this neutral loss can be interpreted to be due to the loss of an acetylhexoside moiety (162 + 42 Da) (Gouveia and Castilho, 2012). The fragment ion at m/z 357 suffered further fragmentation, yielding the fragment ions at m/z 342 $[357–CH_3]^-$, 327 $[357–2CH_3]^-$, 151 $[357–206]^-$, and 136 $[151–CH_3]^-$, which are characteristic of pinoresinol (Han et al., 2007). Therefore this compound, only found in extracts from leaves, was tentatively characterized as pinoresinol-*O*-aceylhexoside.

3.4. Terpenoid saponins

Different saponins were observed in the extracts from leaves and flowers. Compounds 32, 35, 36, and 41 were identified in leaves and flowers, whereas compound 43 was only observed in leaves. The following nomenclature is used: HexA = uronic acid; Hex = hexose; dHex = 6-deoxyhexose, GlcA = glucuronic acid, Gal = galactose, Rha = rhamnose, Agly = aglycone.

Compound 32, with $[M–H]^-$ at m/z 973, was identified as dHex-Hex-HexA-Aglycone D (Pollier et al., 2011) based on the following fragments: 955 $[M–H_2O–H]^-$, 929 $[M–CO_2–H]^-$, 911 $[M–H_2O–CO_2–H]^-$, 827 [M-dHex-H]$^-$, 809 [M-dHex-H_2O–H]$^-$, 783 [M-dHex–CO_2–H]$^-$, 765 [M-dHex-H_2O–CO_2–H]$^-$, 665 [M-dHex-Hex-H]$^-$, 647 [M-dHex-Hex-H_2O–H]$^-$, 629 [M-dHex-Hex-$2H_2O$–H]$^-$, 603 [M-dHex-Hex-H_2O–CO_2–H]$^-$, 557 [M-dHex-Hex-108–H]$^-$, and 489 [Agly–H]$^-$.

Compound 35 exhibited $[M–H]^-$ at m/z 971 and showed the following fragments in MS^2: 953 $[M–H_2O–H]^-$, 927 $[M–CO_2–H]^-$, 909 $[M–H_2O–CO_2–H]^-$, 825 [M-dHex-H]$^-$, 763 [M-dHex-H_2O–CO_2–H]$^-$, 645 [M-dHex-Hex-H_2O–H]$^-$, 627 [M-dHex-Hex-$2H_2O$–H]$^-$, 601 [M-dHex-Hex-$2H_2O$-CO_2–H]$^-$, 555 [M-dHex-Hex-108–H]$^-$, and 487 [Agly–H]$^-$. It was identified as dHex-Hex-HexA-Bayogenin (Pollier et al., 2011).

Compound 36, with $[M–H]^-$ at m/z 957, was characterized as dHex-Hex-HexA-soyasapogenol A (Pollier et al., 2011), and displayed the following fragment ions: 939 $[M–H_2O–H]^-$, 895 $[M–H_2O–CO_2–H]^-$, 811 [M-dHex-H]$^-$, 767 [M-dHex-CO_2–H]$^-$, 749 [M-dHex-H_2O–CO_2–H]$^-$, 631 [M-dHex-Hex-H_2O–H]$^-$, 613 [M-dHex-Hex-$2H_2O$–H]$^-$, 541 [M-dHex-Hex-108–H]$^-$, and 473 [Agly–H]$^-$.

Compound 41 exhibited the deprotonated molecular ion at m/z 941, and presented MS^2 fragment ions at m/z 923 $[M–H_2O–H]^-$, 879 $[M–H_2O–CO_2–H]^-$, 795 [M-Rha-H]$^-$, 751 [M-Rha-CO_2–H]$^-$, 733 [M-Rha-H_2O–CO_2–H]$^-$, 633 [M-Rha-Gal-H]$^-$, 615

[M-Rha-Gal-H_2O–H]$^-$, 597 [M-Rha-Gal-$2H_2O$–H]$^-$, 525 [M-Rha-Gal-108–H]$^-$, and 457 [Agly–H]$^-$. Considering bibliographic data (Pollier et al., 2011), it was identified as 3-Rha-Gal-GlcA-soyasapogenol B.

Compound 43, with $[M–H]^-$ at m/z 939, was identified as dHex-Hex-HexA-soyasapogenol E (Pollier et al., 2011) considering the MS^2 fragment ions at m/z 921 $[M–H_2O–H]^-$, 877 $[M–H_2O–CO_2–H]^-$, 793 [M-dHex-H]$^-$, 749 [M-dHex-CO_2–H]$^-$, 731 [M-dHex-H_2O–CO_2–H]$^-$, 613 [M-dHex-Hex-H_2O–H]$^-$, 595 [M-dHex-Hex-$2H_2O$–H]$^-$, 523 [M-dHex-Hex-108–H]$^-$, and 455 [Agly–H]$^-$.

3.5. Other compounds

Compounds 1, 2, and 3 were characterized as oligosaccharides. Compound 1, with $[M–H]^-$ ion at m/z 683, displayed fragment ions at m/z 503, 341, and 179, which were consistent with the losses of hexoside moieties. The presence of hexoses was confirmed by the fragmentation by MS^4, which exhibited fragment ions at m/z 143, 131, 119, 113, 89, and 71, typical from hexoses (Verardo et al., 2009). Compounds with similar fragmentation have been previously reported as polysaccharides (Brudzynski and Miotto, 2011; Gómez-Caravaca et al., 2008). Compound 2 exhibited an $[M–H]^-$ ion at m/z 457, and suffered the neutral loss of 116 Da (probably malic acid) yielding a fragment ion at m/z 341, which showed typical fragmentation of an hexose disaccharide. Compound 3, with $[M–H]^-$ ion at m/z 473, showed fragment ions at m/z 341 [M–H–132] and 179 [M–H–132–162]. Considering this fragmentation pattern and the MS^4 full spectrum (consistent with hexose), this compound could be tentatively identified as a trisaccharide containing a pentose and two hexoses.

Compound 33, with a $[M–H]^-$ ion at m/z 327 and MS^2 base peak ion at m/z 229, was identified as oxo-dihydroxy-octadecenoic acid (oxo-DHODE), an oxylipin (Spínola et al., 2014; Van Hoyweghen et al., 2014). It was detected in leaves and flowers.

Compound 37 was identified as trihydroxy-octadecenoic acid, considering its $[M–H]^-$ ions at m/z 329 and its fragmentation pattern, previously described in scientific literature (Van Hoyweghen et al., 2014). This oxylipin was detected only in extracts from flowers.

Compound 39 was tentatively characterized as trihydroxy-octadienoic acid based on bibliographic data (Mohn et al., 2009),

due to its deprotonated molecular ion at m/z 327 and fragment ions at m/z 309 and 291. It was detected only in leaves.

4. Conclusion

In this study, a detailed characterization of the phytochemical profile of the methanolic extracts from *B. bituminosa*, from Madeira Archipelago, is presented. Using an HPLC-ESI-MS^n method, more than 40 compounds were detected. All of the compounds (except isoorientin) were identified for the first time in the target plant. Both morphological parts shared a common composition, the leaves being much richer in terms of number of compounds.

About 50% of these compounds corresponded to flavonoids, especially *C*-glycosylated apigenin isomers, although flavonoids from luteolin or kaempferol, among others, were detected. Different terpenoid saponins, lignans, and phenolic acids were also identified. The presence of saponins may indicate potential uses of this plant in hair care products and may be the reason for the traditional use of the plant tincture as hair restorer. Saponins not only have detergent properties, producing stable foams, but they also have antimicrobial activity against several fungi and bacteria (which can be a cause of hair loss), and anti-inflammatory and emollient effects that can sooth the scalp. However, further investigation would be required to study such potential applications for *B. bituminosa* in addition to those currently known.

Acknowledgments

EJLM acknowledges the financial support from Campus de Excelencia Internacional Agroalimentario (ceiA3) and University of Jaén, from Spain. V. Spínola is grateful to Fundação para a Ciência e a Tecnologia (FCT, Portugal) for a Ph.D. grant SFRH/BD/84672/2012. This research was supported by FCT with funds from the Portuguese Government (Project PEst-OE/QUI/UI0674/2011).

References

Azzouzi, S., Zaabat, N., Medjroubi, K., Akkal, S., Benlabed, K., Smati, F., Dijoux-Franca, M.-G., 2014. Phytochemical and biological activities of *Bituminaria bituminosa* L. (Fabaceae). Asian Pac. J. Trop. Med. 7S1, S481–S484.

Barros, L., Dueñas, M., Dias, M.I., Sousa, M.J., Santos-Buelga, C., Ferreira, I.C.F.R., 2012. Phenolic profiles of *in vivo* and *in vitro* grown *Coriandrum sativum* L. Food Chem. 132, 841–848.

Brudzynski, K., Miotto, D., 2011. Honey melanoidins: analysis of the compositions of the high molecular weight melanoidins exhibiting radical-scavenging activity. Food Chem. 127, 1023–1030.

Darias, V., Martín-Herrera, D., Abdala, S., Dela Fuente, D., 2001. Plants used in urinary pathologies in the Canary Islands. Pharm. Biol. 39, 170–180.

Ferreres, F., Silva, B.M., Andrade, P.B., Seabra, R.M., Ferreira, M.A., 2003. Approach to the study of *C*-glycosyl flavones by ion trap HPLC-PAD-ESI/MS/MS: application to seeds of quince (*Cydonia oblonga*). Phytochem. Anal. 14, 352–359.

Fischer, U.A., Carle, R., Kammerer, D.R., 2011. Identification and quantification of phenolic compounds from pomegranate (*Punica granatum* L.) peel mesocarp, aril and differently produced juices by HPLC-DAD-ESI-MSn. Food Chem. 127, 807–821.

Freitas, F., Mateus, M.G., 2013. Plantas E Seus Usos Tradicionais. Parque Natural da Madeira, Madeira.

Gómez-Caravaca, A.M., Verardo, V., Segura-Carretero, A., Caboni, M.F., Fernández-Gutiérrez, A., 2008. Development of a rapid method to determine phenolic and other polar compounds in walnut by capillary electrophoresis–electrospray ionization time-of-flight mass spectrometry. J. Chromatogr. A 1209, 238–245.

Gouveia, S., Castilho, P.C., 2011. Antioxidant potential of *Artemisia argentea* L'Hér alcoholic extract and its relation with the phenolic composition. Food Res. Int. 44, 1620–1631.

Gouveia, S.C., Castilho, P.C., 2012. Phenolic composition and antioxidant capacity of cultivated artichoke: Madeira cardoon and artichoke-based dietary supplements. Food Res. Int. 48, 712–724.

Gouveia, S.C., Castilho, P.C., 2013. *Artemisia annua* L.: essential oil and acetone extract composition and antioxidant capacity. Ind. Crops Prod. 45, 170–181.

Gruz, J., Novák, O., Strnad, M., 2008. Rapid analysis of phenolic acids in beverages by UPLC–MS/MS. Food Chem. 111, 789–794.

Han, J., Ye, M., Guo, H., Yang, M., Wang, B.-R., Guo, D.-A., 2007. Analysis of multiple constituents in a Chinese herbal preparation Shuang-Huang-Lian oral liquid by HPLC-DAD-ESI-MS^n. J. Pharm. Biomed. Anal. 44, 430–438.

Hauck, B., Gallagher, J.A., Morris, S.M., Leemans, D., Winters, A.L., 2014. Soluble phenolic compounds in fresh and ensiled orchard grass (*Dactylis glomerata* L.): a common species in permanent pastures with potential as a biomass feedstock. J. Agric. Food Chem. 62, 468–475.

Jin, Y., Xiao, S., Zhang, F.-F., Xue, Y., Xu, Q., Liang, X.-M., 2008. Systematic screening and characterization of flavonoid glycosides in *Carthamus tinctorius* L. by liquid chromatography/UV diode-array detection/electrospray ionization tandem mass spectrometry. J. Pharm. Biomed. Anal. 46, 418–430.

Jung, E.S., Lee, S., Lim, S.-H., Ha, S.-H., Liu, K.-H., Lee, C.H., 2013. Metabolite profiling of the short-term responses of rice leaves (*Oryza sativa* cv: Ilmi) cultivated under different LED lights and its correlations with antioxidant activities. Plant Sci. 210, 61–69.

Kammerer, D., Carle, R., Schieber, A., 2004. Characterization of phenolic acids in black carrots (*Daucus carota* ssp: *sativus* var. *atrorubens* Alef.) by high-performance liquid chromatography/electrospray ionization mass spectrometry. Rapid Commun. Mass Spectrom. 18, 1331–1340.

Kazuno, S., Yanagida, M., Shindo, N., Murayama, K., 2005. Mass spectrometric identification and quantification of glycosyl flavonoids: including dihydrochalcones with neutral loss scan mode. Anal. Biochem. 347, 182–192.

Kramer, M., Maksylewicz-Kaul, A., Baranski, R., Nothnagel, T., Carle, R., Kammerer, D.R., 2013. Effects of cultivation year and growing location on the phenolic profile of differently coloured carrot cultivars. J. Appl. Bot. Food Qual. 85, 235–247.

March, R.E., Miao, X.-S., 2004. A fragmentation study of kaempferol using electrospray quadrupole time-of-flight mass spectrometry at high mass resolution. Int. J. Mass Spectrom. 231, 157–167.

Martínez-Fernández, D., Walker, D.J., 2012. The effects of soil amendments on the growth of *Atriplex halimus* and *Bituminaria bituminosa* in heavy metal-contaminated soils. Water Air Soil Pollut. 223, 63–72.

Martínez-Fernández, D., Walker, D.J., Romero-Espinar, P., Flores, P., del Río, J.A., 2011. Physiological responses of *Bituminaria bituminosa* to heavy metals. J. Plant Physiol. 168, 2206–2211.

Martínez, S., Correal, E., Real, D., Ortuño, A., del Río, J.A., 2010. *Bituminaria bituminosa*: A Source of Furanocoumarins of Pharmaceutical Interest. In: Awaad, A.S., Govil, J.N., Singh, V.K. (Eds.), Drug Plants. Recent Progress in Medicinal Plants. Studium Press LLC, Houston, pp. 307–322.

Maurich, T., Iorio, M., Chimenti, D., Turchi, G., 2006. Erybraedin C and bitucarpin A, two structurally related pterocarpans purified from *Bituminaria bituminosa*, induced apoptosis in human colon adenocarcinoma cell lines MMR- and p53-proficient and -deficient in a dose-, time-, and structure-dependent fashion. Chem. Biol. Interact. 159, 104–116.

Mohn, T., Plitzko, I., Hamburger, M., 2009. A comprehensive metabolite profiling of *Isatis tinctoria* leaf extracts. Phytochemistry 70, 924–934.

Ozarowski, M., Mikolajczak, P.L., Bogacz, A., Gryszczynska, A., Kujawska, M., Jodynis-Liebert, J., Piasecka, A., Napieczynska, H., Szulc, M., Kujawski, R., Bartkowiak-Wieczorek, J., Cichocka, J., Bobkiewicz-Kozlowska, T., Czerny, B., Mrozikiewicz, P.M., 2013. *Rosmarinus officinalis* L. leaf extract improves memory impairment and affects acetylcholinesterase and butyrylcholinesterase activities in rat brain. Fitoterapia 91, 261–271.

Pecetti, L., Tava, A., Pagnotta, M.A., Russi, L., 2007. Variation in forage quality and chemical composition among Italian accessions of *Bituminaria bituminosa* (L.) Stirt. J. Sci. Food Agric. 87, 985–991.

Permender, R., Hema, C., Sushila, R., Dharmender, R., Vikash, K., 2010. Antidiabetic potential of fabaceae family: an overview. Curr. Nutr. Food Sci. 6, 161–175.

Pollier, J., Morreel, K., Geelen, D., Goossens, A., 2011. Metabolite profiling of triterpene saponins in *Medicago truncatula* hairy roots by liquid chromatography Fourier transform ion cyclotron resonance mass spectrometry. J. Nat. Prod. 74, 1462–1476.

Press, J.R., Short, M.J., 2001. The Flora of Madeira. Natural History Museum, London.

Qiao, X., He, W.-N., Xiang, C., Han, J., Wu, L.-J., Guo, D.-A., Ye, M., 2011. Qualitative and quantitative analyses of flavonoids in *Spirodela polyrrhiza* by high-performance liquid chromatography coupled with mass spectrometry. Phytochem. Anal. 22, 475–483.

Rivera, D., Obón, C., 1995. The ethnopharmacology of Madeira and Porto Santo Islands, a review. J. Ethnopharmacol. 46, 73–93.

Santos, J., Oliveira, M.B.P.P., Ibáñez, E., Herrero, M., 2014. Phenolic profile evolution of different ready-to-eat baby-leaf vegetables during storage. J. Chromatogr. A 1327, 118–131.

Simirgiotis, M.J., Schmeda-Hirschmann, G., Bórquez, J., Kennelly, E.J., 2013. The *Passiflora tripartita* (banana passion) fruit: a source of bioactive flavonoid *C*-glycosides isolated by HSCCC and characterized by HPLC-DAD-ESI/MS/MS. Molecules 18, 1672–1692.

Slimestad, R., 2003. Flavonoids in buds and young needles of *Picea*, *Pinus and Abies*. Biochem. Syst. Ecol. 31, 1247–1255.

Spínola, V., Llorent-Martínez, E.J., Gouveia, S., Castilho, P.C., 2014. *Myrica faya*: a new source of antioxidant phytochemicals. J. Agric. Food Chem. 62, 9722–9735.

Sternberg, M., Gishri, N., Mabjeesh, S.J., 2006. Effects of grazing on *Bituminaria bituminosa* (L.) Stirton: a potential forage crop in mediterranean grasslands. J. Agron. Crop Sci. 192, 399–407.

Tava, A., Pecetti, L., Ricci, M., Pagnotta, M.A., Russi, L., 2007. Volatile compounds from leaves and flowers of *Bituminaria bituminosa* (L.) Stirt. (Fabaceae) from Italy. Flavor Fragance J. 22, 363–370.

Van Hoyweghen, L., De Bosscher, K., Haegeman, G., Deforce, D., Heyerick, A., 2014. In vitro inhibition of the transcription factor NF-B and cyclooxygenase by bamboo extracts. Phytother. Res. 28, 224–230.

Ventura, M.R., Castañón, J.I.R., Pieltain, M.C., Flores, M.P., 2004. Nutritive value of forage shrubs: *Bituminaria bituminosa*, *Rumex lunaria*, *Acacia salicina*, *Cassia sturtii* and *Adenocorpus foliosus*. Small Ruminant Res. 52, 13–18.

Verardo, G., Duse, I., Callea, A., 2009. Analysis of underivatized oligosaccharides by liquid chromatography/electrospray ionization tandem mass spectrometry with post-column addition of formic acid. Rapid Commun. Mass Spectrom. 23, 1607–1618.

Walker, D.J., Martínez-Fernández, D., Correal, E., Romero-Espinar, P., del Río, J.A., 2012. Accumulation of furanocoumarins by *Bituminaria bituminosa* in relation to plant development and environmental stress. Plant Physiol. Biochem. 54, 133–139.

Waridel, P., Wolfender, J.-L., Ndjoko, K., Hobby, K.R., Major, H.J., Hostettmann, K., 2001. Evaluation of quadrupole time-of-flight tandem mass spectrometry and ion-trap multiple-stage mass spectrometry for the differentiation of *C*-glycosidic flavonoid isomers. J. Chromatogr. A 926, 29–41.

Ye, M., Yan, Y., Guo, D.-A., 2005. Characterization of phenolic compounds in the Chinese herbal drug Tu-Si-Zi by liquid chromatography coupled to electrospray ionization mass spectrometry. Rapid Commun. Mass Spectrom. 19, 1469–1484.

Zhang, M., Duan, C., Zang, Y., Huang, Z., Liu, G., 2011. The flavonoid composition of flavedo and juice from the pummelo cultivar (*Citrus grandis* (L.) Osbeck) and the grapefruit cultivar (*Citrus paradisi*) from China. Food Chem. 129, 1530–1536.